

Spectral reconstruction of the flash X-ray generated by Dragon-I LIA based on transmission measurements Postprint

Authors: CAO Jing, Xiao Rui, CHEN Nan, CAO Hong-Rui, YIN Ze-Jie

Date: 2023-06-18T00:00:00+00:00

Abstract

The Dragon-I linear induction accelerator (LIA) at the China Academy of Engineering Physics generates 20 MeV flash X-rays primarily for radiography applications in fluid dynamics. Its spectral information is of considerable importance for diagnostic X-ray imaging applications; however, due to its short pulse duration and high radiation intensity, direct measurement is not feasible. In this work, we propose a novel method based on transmission measurements to reconstruct the flash X-ray spectrum. Pure iron cylinders were employed as attenuation material, with alanine dosimeters attached to their rear surfaces to record the dose following varying degrees of attenuation. The iterative least-squares method was utilized to unfold the spectrum, while the Geant4 Monte Carlo code was employed to simulate the X-ray spectrum. The unfolded spectrum and the simulated spectrum exhibit a high degree of consistency, with a reduced chi-square value of 0.044. This demonstrates that the method is reliable for estimating megavoltage high-intensity X-ray spectra.

Full Text

Preamble

Spectral Reconstruction of the Flash X-Ray Generated by Dragon-I LIA Based on Transmission Measurements

CAO Jing (曹靖)^{1,2}, XIAO Rui (肖睿)^{1,2}, CHEN Nan (陈楠)³, CAO Hong-Rui (曹宏睿)^{1,2}, and YIN Ze-Jie (阴泽杰)^{1,2,†}

¹State Key Laboratory of Particle Detection and Electronics, University of Science and Technology of China, Hefei 230026, China

²Department of Modern Physics, University of Science and Technology of China, Hefei 230026, China

³Institute of Fluid Physics, China Academy of Engineering Physics, Mianyang 621900, China

(Received August 29, 2014; accepted in revised form October 6, 2014; published online August 20, 2015)

The Dragon-I linear induction accelerator (LIA) at China Academy of Engineering Physics generates 20 MeV flash X-rays mainly for radiography applications in fluid dynamics. Its spectral information is quite important for diagnostic X-ray imaging applications, but because of its short pulse and great radiation intensity, direct measurement is impossible. In this work, we propose a new method based on transmission measurements to obtain the flash X-ray spectrum. Pure iron cylinders were used as attenuation material, and alanine dosimeters were attached on their rear bottom to record the dose after different degrees of attenuation.

An iterative least squares method was used to unfold the spectrum, while Geant4 Monte Carlo code was used to simulate the X-ray spectrum. The unfolded spectrum and the simulated spectrum have a high degree of consistency, with the reduced chi-square value of 0.044. This shows that the method is reliable in estimating megavoltage high-intensity X-ray spectra.

Keywords: X-ray spectra, Dragon-I, Spectral reconstruction, Transmission measurements, Geant4

DOI: 10.13538/j.1001-8042/nst.26.040403

Introduction

The Dragon-I LIA at China Academy of Engineering Physics (CAEP) can produce high-quality 20 MeV electron beams with a beam current of over 2.5 kA, pulse width of 60 ns, and focal spot size of about 1.5 mm. By bombarding high-Z targets, it can generate high-intensity flash X-rays of up to 20 MeV via bremsstrahlung. These flash X-rays are quite effective for radiography applications in fluid dynamics research [1, 2].

The flash X-ray spectrum is an important parameter for X-ray imaging diagnostics such as beam-hardening correction, dose deposition calculation, dual-energy material detection, and related applications. However, due to the short pulse width and great radiation intensity, the X-ray spectrum cannot be measured by traditional methods. It is typically obtained either from simulation or measured with large error that depends heavily on an assumed spectrum [3-5]. In this work, we propose a new method to accurately measure the X-ray spectrum based on transmission measurements.

II. Method

Traditional multichannel spectroscopy is not suitable for high-intensity X-rays. Because of severe pulse pile-up, the pulse height information representing photon

energy cannot be determined correctly. The X-rays are emitted in just tens of nanoseconds, and the electronics system cannot acquire all pulse information in such a short time. Thus, indirect methods must be used for high-intensity X-ray spectroscopy. Currently, transmission measurement is a principal method for measuring high-intensity X-ray spectra [6-13]. This method is relatively straightforward and can be applied across a wide range of photon energies.

For n layers of pure attenuation materials, when X-rays traverse one of them, the transmission function is:

$$I(h) = \int_{E_{\min}}^{E_{\max}} X(E) E e^{(-\mu(E)h)} dE,$$

where $I(h)$ is the intensity of the transmitted X-rays, E is X-ray energy, E_{\max} and E_{\min} are the maximum and minimum energy, $X(E)$ is the photon counting spectrum, $\mu(E)$ is the linear attenuation coefficient of X-rays in the material, and h is the thickness of the material layer. By defining $R(E, h) = E e^{-\mu(E)h}$, Eq. (1) can be written as:

$$I(h) = \int_{E_{\min}}^{E_{\max}} X(E) R(E, h) dE.$$

After discretization, Eq. (2) becomes:

$$I(h_j) = \sum_{i=1}^m R(i, j) X_j \quad (i = 1, 2, \dots, m; j = 1, 2, \dots, n),$$

where $R(i, j)$ is the response matrix, and m is the number of discrete points of the X-ray counting spectrum X . $R(i, j)$ can be calculated from the X-ray linear attenuation coefficients and thickness, and $I(h)$ can be measured. The problem now is how to solve for the spectrum X through the known R and $I(h)$ in the linear system of Eq. (3).

However, Eq. (3) is ill-conditioned, and usually n is far less than m , limited by experimental conditions. It cannot be solved directly. In this work, we unfold the spectrum based on the MLEM algorithm [14]; the goal is to obtain the spectrum that best matches the measured data. The squared residual error $S = \|I - RX\|^2$ must be minimized. Based on the least squares method, this can be transformed to the regularized equations:

$$R^T I = R^T R X,$$

where R^T is the transpose matrix of R . Assuming $N = R^T I$ and $A = R^T R$, we have:

$$N = AX.$$

Iteration methods can be used to solve Eq. (6) to obtain the X-ray photon counting spectrum X .

III. Experimental

A. Simulation

The process of 20 MeV electron beams bombarding tantalum targets to produce high-intensity flash X-rays can be simulated by Monte Carlo particle transport simulation tools such as Geant4 [15-17], MCNP [18], and FLUKA [19], based on the geometry of the real experimental environment (Fig. 1(a)). In this paper, Geant4 (version 10.00.p02) was used. The simulation was performed with 5×10^8 electrons at 20 MeV. The X-ray photons were collimated by stainless steel collimators. Some of them entered the detection area, and the counting spectrum is shown in Fig. 1(b).

The results show that the counts are mainly in the energy range of < 5 MeV, above which they change slowly. Some fine structure can be seen at 0.511 MeV and below. This helps the X-ray spectrum reconstruction. The green and red lines represent trajectories of photons and electrons, respectively.

B. Measurement

Pure iron was used as attenuation material and the attenuated dose was measured by alanine dosimeters. An epoxy frame was used to hold 12 iron cylinders with lengths of 2.1, 6.0, 10.3, 15.0, 20.2, 26.2, 33.1, 41.2, 51.2, 64.0, 82.2, and 113.3 mm (Fig. 2). The alanine dosimeters were attached to the rear bottom of each iron cylinder. Alanine dosimeters are not energy-dependent above 100 keV, making them suitable for MeV flash X-ray detection. Their dose readings exhibit good linearity over a wide dose range of $10 - 2 \times 10^5$ Gy, with an overall measurement error of less than 5%. These characteristics are helpful for the spectrum unfolding algorithm [20].

Dosimetry measurements of the high-intensity flash X-rays penetrating Fe cylinders of different lengths were performed on the Dragon-I LIA at CAEP. ESR (electron spin resonance) reading of the alanine dosimeters was done at CUST. The results are shown in Table 1. The alanine dosimeters for the Fe tablets with lengths of 2.1 and 6.0 mm show extraordinarily high dose readings, as these two Fe cylinders were too short to stop the electrons escaping from the PMMA shielding. Therefore, only the 10 dose readings for the Fe tablets longer than 10 mm were used for spectrum unfolding.

IV. Response Matrix

To solve the discrete X-ray spectrum $X_i (i = 1, 2, \dots, m)$ in Eq. (3), accuracy of the response matrix $R(i, j)$ is important. The definition of $R(E, h) = Ee^{-\mu(E)h}$ in Section II concerns only the attenuated incident X-rays. For high-energy X-rays induced by 20 MeV electron beams, however, the situation is far more complex. The alanine dosimeters on the rear bottom of the Fe cylinders were irradiated not only by the incident X-rays, but also by scattered X-rays and electrons generated by the electron pair effect, a photon-material reaction of X-rays with energy ≥ 1.02 MeV. Therefore, the response matrix $R(i, j)$ must be re-defined. Theoretical calculation of the real $R(i, j)$ is difficult, but the Monte Carlo method offers an easy way to calculate it.

If the incident X-ray photons are mono-energetic, one has the following equation:

$$R(E_0, h) = I(h)/N,$$

where N is the number of incident photons at energy E_0 and $I(h)$ stands for the transmitted X-ray intensity, which can be detected by the alanine dosimeters. The Geant4 simulation was conducted with mono-energetic photons at 30 discrete energy points from 0.2 MeV to 20 MeV, in order to calculate energy deposition in alanine dosimeters on the rear bottom of the 10 Fe cylinders with lengths of 10.3–113.3 mm. The energy depositions were converted to absorbed doses, and Eq. (7) was used to obtain the response of the 10 alanine dosimeters to a particular energy of the X-ray photons. As Fig. 1(b) shows, the simulated X-ray yield changes little in the energy range above 5 MeV, and the main peak is below 5 MeV. Thus we selected 25 points in the < 5 MeV region (i.e., 0.2, 0.4, 0.6, ..., 4.8 MeV) and 5 points in the > 5 MeV region (i.e., 6, 8, 10, 15, 20 MeV). A total of 10^9 X-ray photons were simulated for each energy point, and the calculated response matrix was plotted in Fig. 3.

V. Results

Using Eq. (3), we unfolded the X-ray spectrum with the dose readings in Table 1, the response matrix (Fig. 3), and the iterative MLEM unfolding algorithm mentioned in Section II. The results are shown in Fig. 4, together with the simulated spectrum from Fig. 1(b). It can be seen that the reconstructed spectrum is in close proximity to the simulated spectrum. The reduced chi-square was calculated as 0.044. The difference between the two spectra can be reasoned as follows. First, the Geant4 simulation was done with simplified experimental conditions, and each parameter was chosen ideally (e.g., the incident electrons are all exactly 20 MeV energy). However, the real electron beams generated by the LIA have an energy spread around 20 MeV, and it is hard to take this factor into account in the simulation. Imperfection in the unfolding algorithm and in dosimetry may be another source of errors. In this work, we unfolded the 30-point spectrum from dose readings of only 10 alanine dosimeters.

VI. Conclusion

It is quite difficult to obtain spectral information of high-intensity flash X-rays because of their short pulse width and great radiation dose. Based on transmission measurements, we propose a new method to obtain the X-ray spectrum generated by Dragon-I LIA. A PMMA frame was designed to hold all the attenuation materials and dosimeters. The reconstructed spectrum has a high degree of consistency with the simulated spectrum. These results prove that the method is reliable for estimating high-intensity flash X-ray spectra.

The work needs to be improved in several ways. More iron cylinders should be fixed in the PMMA frame for better quality of spectrum unfolding. Different kinds of attenuation materials should be used, such as copper, aluminum, and beryllium, and more experiments should be done with each attenuation material. In this work, we used only 30 discrete energy points, focused in the 0-5 MeV energy region. In future work, we will unfold the spectrum with more discrete energy points across the entire 0-20 MeV energy range.

References

- [1] Deng J J, Ding B B, Wang H C, et al. Physical design of the Dragon-I linear induction accelerator. *High P Lase Part Beam*, 2003, 15: 502-504. (in Chinese)
- [2] Ding B N, Deng J J, Wang H C, et al. Dragon-I linear induction election accelerator. *High Energ Phys Nucl Phys*, 2005, 29: 604-610. (in Chinese) DOI: 10.3321/j.issn:0254-
- [3] Delgado V. Determination of x-ray spectra from Al attenuation data by imposing a prior physical features of the spectrum: Theory and experimental validation. *Med Phys*, 2009, 36: 142-148. DOI: 10.1118/1.3031117
- [4] Li C G, Deng J J, Li Q, et al. Design and application of an integrative device for diagnosing high-energy X-ray source. *Nucl Tech*, 2011, 34: 433-436. (in Chinese)
- [5] Wang Y, Li Q and Jiang X G. Monte Carlo simulations for 20 MV X-ray spectrum reconstruction of a linear induction accelerator. *Chinese Phys C*, 2012, 36: 861-866. DOI: 10.1088/1674-1137/36/9/012
- [6] Silberstein L. Determination of the spectral composition of X-ray radiation from filtration data. *J Opt Soc Am*, 1932, 22: 265-280. DOI: 10.1364/JOSA.22.000265
- [7] Waggener R G, Blough M M, Terry J A, et al. X-ray spectra estimation using attenuation measurements from 25 kVp to 18 MV. *Med Phys*, 1999, 26: 1269-1278. DOI: 10.1118/1.598622
- [8] Stampanoni M, Fix M, Francois P, et al. Computer algebra for x-ray spectral reconstruction between 6 and 25 MV. *Med Phys*, 2001, 28: 325-327. DOI: 10.1118/1.1350585

- [9] Lei J R, Ran S Y, Yuan Y G, et al. Reconstruction of 12 MV bremsstrahlung spectra from measured transmission data. Nucl Sci Tech, 2003, 14: 138-143.
- [10] Shimozato T, Tabushi K, Kitoh S, et al. Calculation of 10 MV X-ray spectra emitted by a medical linear accelerator using the BFGS quasi-Newton method. Phys Med Biol, 2007, 52: 515-523. DOI: 10.1088/0031-9155/52/2/014
- [11] Manciu M, Manciu F S, Vulcan T, et al. Robust megavoltage x-ray spectra estimation from transmission measurements. J X-Ray Sci Technol, 2009, 17: 85-99. DOI: 10.3233/XST-2009-
- [12] Duan X H, Wang J, Yu L F, et al. CT scanner x-ray spectrum estimation from transmission measurements. Med Phys, 2011, 38: 993-997. DOI: 10.1118/1.3547718
- [13] Ali E S M and Rogers D W O. An improved physics-based approach for unfolding megavoltage bremsstrahlung spectra using transmission analysis. Med Phys, 2012, 39: 1663-1675. DOI: 10.1118/1.3687164
- [14] Zhao J W and Su W N. An iterative image reconstruction algorithm for SPECT. Nucl Sci Tech, 2014, 25: 030302. DOI: 10.13538/j.1001-8042/nst.25.030302
- [15] Agostinelli S, Allison J, Amako K, et al. Geant4-a simulation toolkit. Nucl Instrum Meth A, 2003, 506: 250-303. DOI: 10.1016/S0168-9002(03)01368-8
- [16] Kadri O, Alnafea M A and Shamma K. Computation and parameterization of normalized glandular dose using Geant4. Nucl Sci Tech, 2015, 26: 030303. DOI: 10.13538/j.1001-8042/nst.26.030303
- [17] Cao J, Jiang X F, Jiang C Y, et al. Calculation of response function for bonner sphere spectrometer based on Geant4. Plasma Sci Technol, 2015, 17: 80-83. DOI: 10.1088/1009-0630/17/1/15
- [18] Li L, Li X Y, Huang W, et al. Study on improving MCNP computational efficiency of dose rate for a single-rack cobalt irradiation facility. Nucl Tech, 2015, 38: 030201. (in Chinese) DOI: 10.11889/j.0253-3219.2015.hjs.38.030201
- [19] Cao Z, Ruan X C, Meng B D, et al. Determination of dosimetric characteristics for 125I seed source with FLUKA code. Nucl Sci Tech, 2014, 25: 060601. DOI: 10.13538/j.1001-8042/nst.25.060601
- [20] Regulla D F and Deffner U. Dosimetry by ESR Spectroscopy of Alanine. Int J Appl Radiat Isot, 1982, 33: 1101-1114. DOI: 10.1016/0020-708X(82)90238-1

Figures

Source: ChinaXiv – Machine translation. Verify with original.

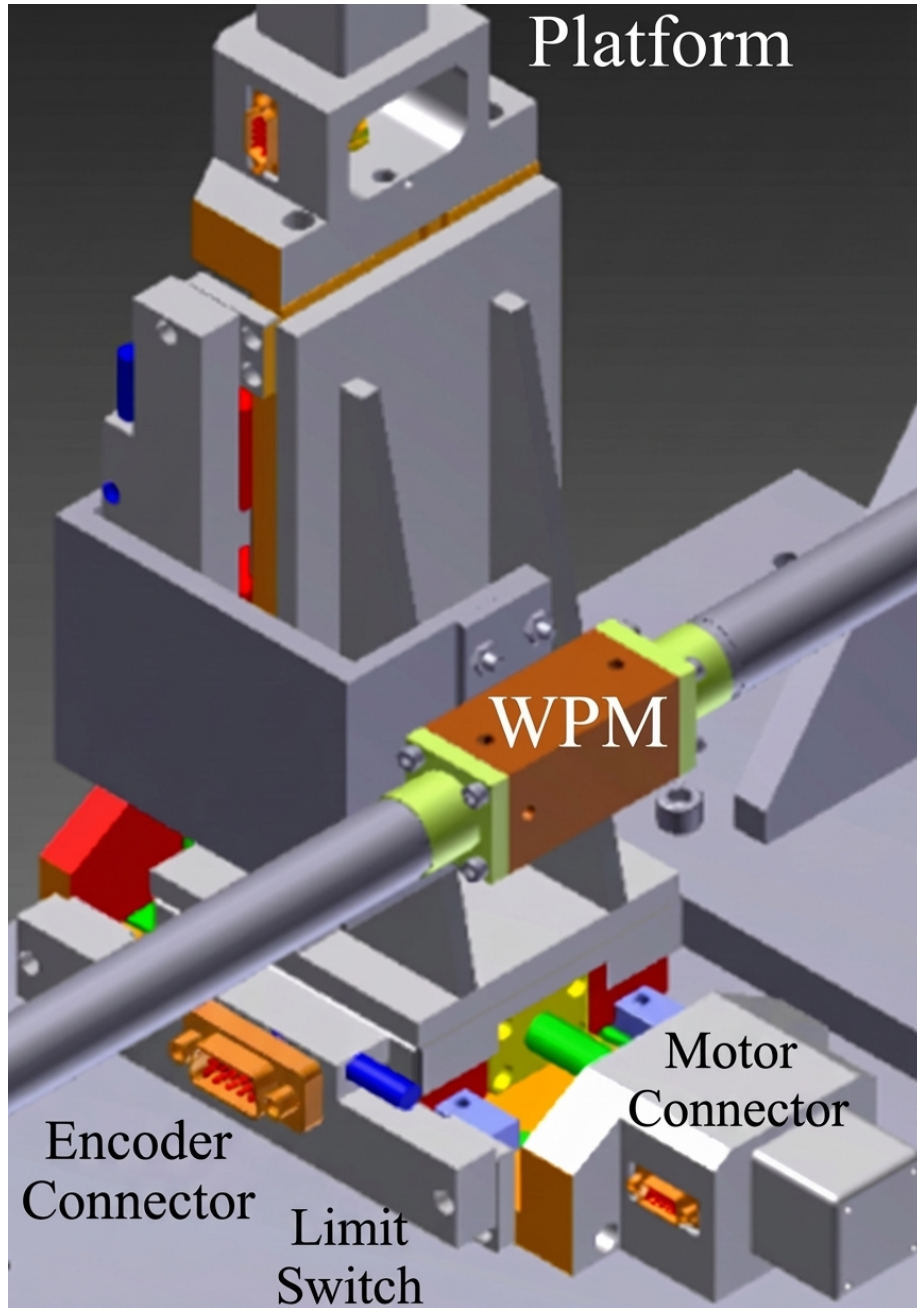


Figure 1: Figure 3

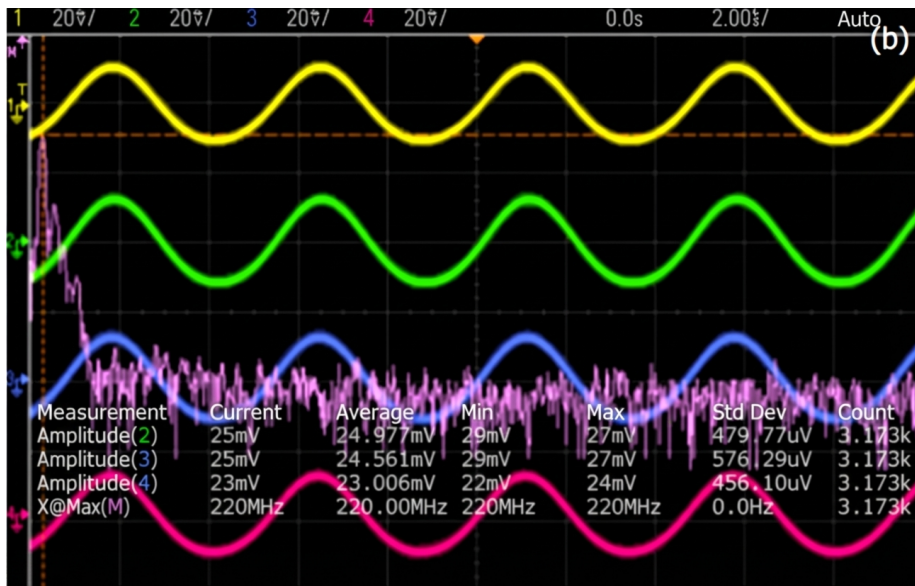


Figure 2: Figure 5